Journal of Catalysis 258 (2008) 170–176

Contents lists available at ScienceDirect

Journal of Catalysis

www.elsevier.com/locate/jcat

# Ruthenium at work in Ru-hydroxyapatite during the aerobic oxidation of benzyl alcohol: An *in situ* ATR-IR spectroscopy study

Cecilia Mondelli [a], Davide Ferri [b], Alfons Baiker [a,*]

[a] *Department of Chemistry and Applied Biosciences, ETH Zurich, Hönggerberg HCI, CH-8093 Zurich, Switzerland*
[b] *Laboratory for Solid State Chemistry and Catalysis, Empa, Ueberlandstrasse 129, CH-8600 Dübendorf, Switzerland*

ARTICLE INFO

*Article history:*
Received 22 April 2008
Revised 5 June 2008
Accepted 5 June 2008
Available online 10 July 2008

*Keywords:*
Ruthenium
Hydroxyapatite
Alcohol oxidation
Liquid phase
*In situ* ATR-IR spectroscopy

ABSTRACT

The structure of Ru in Ru-substituted hydroxyapatite (RuHAp) has been investigated using infrared spectroscopy in the attenuated total reflection mode (ATR-IR). Oxidation–reduction cycles, $^{12}CO$ and $^{13}CO$ adsorption have been used to determine the state of Ru in the presence of cyclohexane solvent. The spectroscopic data support the existence of a hydrated $RuO_x$-like phase, which is identified by overtone signals of Ru–O bonds at ca. 1850 $cm^{-1}$ and is likely organized as a two-dimensional phase on the apatite. This phase coexists with isolated $Ru^{3+}$ cations likely located in the hardly accessible channels of the apatite structure. The $RuO_x$-like phase is shown to be highly reactive at the solid–liquid interface and exhibits a number of carbonyl species upon CO adsorption. The relevance of the $RuO_x$-like phase for the liquid-phase aerobic oxidation of benzyl alcohol has been investigated under close to reaction conditions. Although weak signals of benzaldehyde indicate that conversion is likely low under flow conditions, their presence makes the results relevant to draw structure–activity relationships. Blocking of accessible Ru sites using CO prior to reaction reveals that only selected CO species on the hydrated $RuO_x$-like phase are depleted when reaction occurs. The likely formation of $HCO_3^-$ in the absence of the alcohol indicates that benzyl alcohol oxidation and $HCO_3^-$ formation may occur on similar Ru sites providing evidence that these sites are located on the $RuO_x$ phase.



## 1. Introduction

Hydroxyapatite [HAp, $Ca_{10}(PO_4)_6(OH)_2$] has generated great interest in the past years as stable and recyclable support for the preparation of heterogeneous catalysts employed in organic synthesis [1–8]. The partial replacement of $Ca^{2+}$-ions in the lattice of hydroxyapatite with 1–4 valent metal ions affords different classes of materials [9–13]. Among these, Ru-exchanged HAp exhibits excellent catalytic performance in a wide range of chemical transformations, mainly partial oxidation of alcohols [14–18], amines [19], and organosilanes [20] with molecular oxygen, Diels–Alder and aldol condensation reactions and oxidative cleavage of alkenes [21–23].

The remarkable catalytic activity of RuHAp for alcohol oxidation is related to its bifunctional character: the redox activity of the Ru sites and the basic sites in the apatite lattice that provide additional dehydrogenation activity. Moreover, it is claimed that monomeric metal species can be created on apatites which is an attractive issue for single-site catalysis [21]. Nevertheless, the nature of the active site in Ru-containing hydroxyapatites is still matter of debate [15,24,25]. Since the preparation method involves a number of complex phenomena as ion exchange by diffusion, adsorption and dissolution–reprecipitation [14], it is likely that Ru appears as a combination of species of different chemical and structural nature. The presence of dihydroxo-ruthenium oxide species on the RuHAp system has been demonstrated using *in situ* EXAFS during benzyl alcohol oxidation. The absence of chlorine as possible residue of the precursor salt was confirmed for low-loading materials (<4 wt% Ru) [16,18], whereas chlorine was found to coordinate to Ru and Pd for higher loadings [15,26]. DRIFT spectroscopy of CO adsorption revealed the presence of a (likely) two-dimensional hydrated $Ru^{3+}$-oxide-like phase as well as isolated, monomeric $Ru^{3+}$ cations. Interestingly, the marked intensity changes of the overtones of the stretching vibrations of $Ru^{4+}$–O and $Ru^{3+}$–O under different gas-phase treatments, revealed a high redox activity of the surface metal oxidic phase. STEM images of the as prepared sample revealed Ru-containing aggregates of about 1–3 nm finely dispersed on the support material, which were ascribed to the surface $RuO_x$ phase. EXAFS and XPS analysis of the catalyst confirmed the oxidized state of Ru [16]. On the contrary, the ionic $Ru^{3+}$ species located on the outer surface and in the channel of the apatite structure did not produce any detectable pattern (Fig. 1a) [27]. STEM micrographs taken after benzyl alcohol oxidation indicated no structural changes [27]. Promotion of

* Corresponding author.
*E-mail address:* baiker@chem.ethz.ch (A. Baiker).

0021-9517/$ – see front matter 
doi:10.1016/j.jcat.2008.06.011

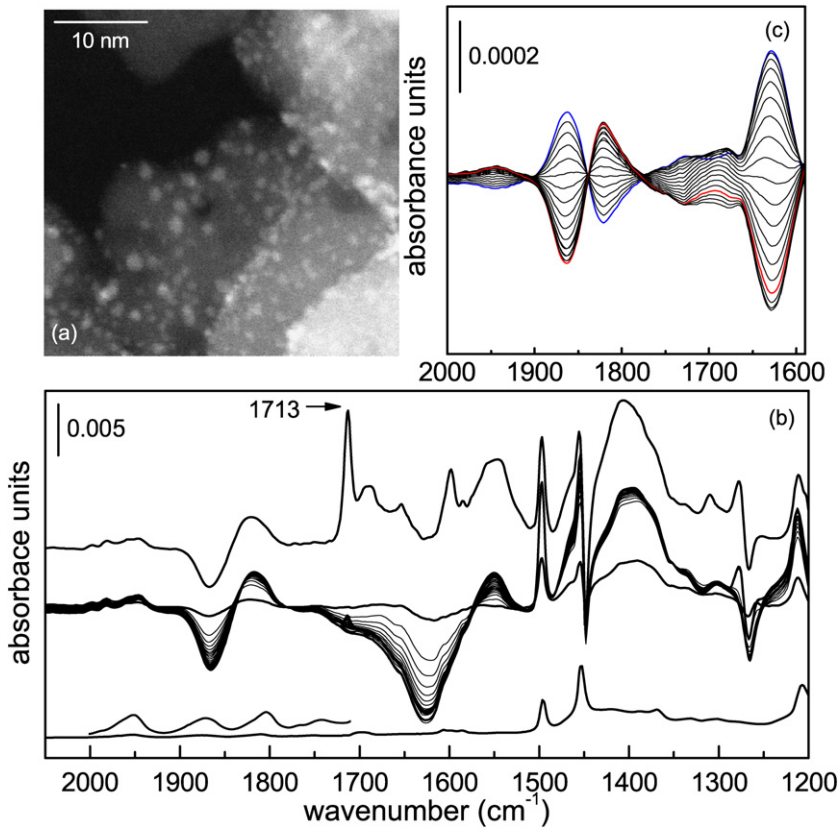


**Fig. 1.** (a) HAADF-STEM image of the as prepared RuHAp. (b) Time-dependent ATR-IR spectra of the as prepared RuHAp in contact with an Ar-saturated benzyl alcohol solution (0.02 M) and (offset) the ATR-IR spectrum of RuHAp after 1 h contact with the reaction mixture under stopped-flow conditions; ATR-IR spectrum of neat benzyl alcohol (bottom). (c) Selected phase-resolved spectra with 10° phase angle difference obtained during a MES experiment in which the feed was periodically changed between $H_2$- and $O_2$-saturated solvent. Conditions: cyclohexane solvent, benzyl alcohol 0.02 M, $O_2$ ($H_2$), 333 K, 0.6 ml/min flow rate.

RuHAp by cobalt ions resulted in the deposition of Ru on the external surface of HAp and in the preferential inclusion of Co within the HAp channels [16]. On the basis of these evidences, the hydrated $Ru^{3+}$-oxide nanoparticles identified on HAp have been indicated as feasible active sites for the catalytic oxidation of alcohols [27].

The present work aims at establishing a realistic link between catalytic and structural properties of the heterogeneous material as immersed in the liquid phase and at refining the existing knowledge, in terms of catalyst structure. The spectroscopic investigation reported in this study is carried out under experimental conditions relevant for the catalysis. The catalytic system is monitored at work by means of infrared spectroscopy in the internal reflection geometry (ATR-IR) [28,29]. This technique allows enhancing sensitivity towards the solid–liquid interface and constitutes a tool of choice for studying at a molecular level processes occurring at the catalyst–solution boundary under realistic reaction conditions [30–37]. Of particular interest for this study is the behavior of the spectral signature of the $RuO_x$ phase under these conditions and consequently its relevance and involvement in the catalysis.

## 2. Experimental

### 2.1. Materials

The Ru-hydroxyapatite (RuHAp) catalyst was prepared as described elsewhere [16]. Briefly, the ruthenium metal was introduced by shaking stoichiometric HAp with a 6.7 mM solution of $RuCl_3$ hydrate (ABCR, 36% Ru, 99.9%) in water for 10 min. The solid was filtered off and washed with deionized water. The catalyst was dried under vacuum at 80 °C for 8 h. The Ru–alumina catalyst was similarly prepared following the same procedure but with $Al_2O_3$. The effective loading of Ru was measured using AAS after acid solubilization of the catalysts and amounted to about 2.8 and 1.2% respectively. Characterization of RuHAp has been extensively reported in Refs. [14,16,17,27] with respect, for example, to the state of Ru in the as prepared catalyst and after reaction, the exchange of Ru for Ca and the morphology of the catalyst, among other properties.

### 2.2. Attenuated total reflection infrared spectroscopy

A thin powder layer of 5 mg of RuHAp was prepared by depositing an aqueous slurry (high purity water, Merck) of the catalytic material onto the large face of the trapezoidal ZnSe internal reflection element (IRE, bevel of 45°, 52 × 20 × 2 mm, Crystran Ltd.). For this purpose, the ATR prism was inserted in a mask in order to expose to the suspension only the geometric area of the channel (ca. 40 × 7 mm). After evaporation in air, the catalyst film was dried at 50 °C for 8 h under vacuum. Despite this treatment, the resulting powder film is partially hydrated.

The detailed procedure of the ATR-IR measurement has been described elsewhere [38]. Briefly, a home-built stainless steel flow-through cell serving as a continuous-flow reactor was mounted onto the ATR attachment (Optispec) within the FT-IR spectrometer (IFS-66/S, Bruker Optics) equipped with an MCT detector cooled with liquid nitrogen. All ATR-IR spectra were recorded by averaging 200 scans at 4 $cm^{-1}$ resolution. Where required, spectra were corrected to compensate for the absorption of atmospheric water. The cell was kept at 333 K throughout the measurements using a thermostat.

Cyclohexane solvent (Acros, >99%) and the benzyl alcohol (Aldrich, >99%, 20 mM) solution saturated with different gases were provided from two glass bubble reservoirs. Two pneumatically activated Teflon valves installed at the inlets of the cell were used to select the appropriate solution from a reservoir. The flows were regulated at a liquid flow rate of 0.60 ml/min using a peristaltic pump (Reglo 100, Ismatec) located after the cell. Stainless steel tubing was used throughout.

The following protocol was used for the alcohol oxidation experiments. After Ar-saturated cyclohexane was admitted to the two flow channels for 60 min, the reaction was started by supplying the solution of benzyl alcohol saturated with Ar to the catalysts. After 30 min the flow was stopped for ca. 30 min. Then Ar was replaced by air in the same reservoir and the air-saturated solution of the alcohol was contacted with the catalyst coating for ca. 30 min. Then the flow was stopped for 30 min again. In case of $^{12}CO$ (10 vol% CO/Ar, PANGAS) and $^{13}CO$ (99 at% $^{13}C$, 12 at% $^{18}O$, Linde, PANGAS) adsorption from the liquid phase, CO-saturated cyclohexane was fed to the cell.

Modulation excitation spectroscopy (MES) [39,40] measurements were performed by periodically changing the reactants concentration. After the stabilization phase under Ar-saturated solvent, liquids from the two bubble tanks were alternately admitted to the cell by switching the computer controlled valves within the data acquisition loop of the measurement program. The system was allowed to reach a quasi-stationary state during two full modulation periods. Data were then averaged over six modulation periods. Within one modulation period (588.6 s), 60 spectra were recorded by co-adding 50 scans per spectrum. The relatively long duration of the period was necessary to better identify the signals arising from the kinetically rather slow processes occurring at the solid–liquid interface in the ATR flow-through cell. The time-resolved single beam spectra were transformed into absorbance spectra using the average of all single beam spectra as the background. These time resolved spectra were then elaborated using the demodulation function to obtain phase-demodulated spectra [39–41].

### 2.3. Batch reactor catalytic measurements

Catalytic tests were performed with oxygen at 1 bar and 333 K using a solution of 1 mmol alcohol in 10 ml toluene or cyclohexane and 60 mg of catalyst [14,17]. Selectivity and conversion were determined by gas chromatography (Thermo Quest Trace 2000, equipped with an HP-FFAP capillary column and a flame ionization detector).

## 3. Results and discussion

The spectra obtained upon contacting the RuHAp film with the Ar-saturated benzyl alcohol solution in cyclohexane (dehydrogenation conditions, Fig. 1b) display the typical features of dissolved and adsorbed alcohol (1497, 1395 and 1215 $cm^{-1}$, Table 1) [42]. The depletion of the signal at 3656 $cm^{-1}$ (not shown), related to the stretching mode of surface hydroxyl groups [43], accompanying the growth of a broad signal below 3500 and 3000 $cm^{-1}$, indicates that these sites are strongly perturbed by the presence of the alcohol and by the surface processes occurring on the RuHAp surface. In contrast, a weak positive signal at 3568 $cm^{-1}$ suggests that the contribution from OH-groups located within channels of the HAp structure is negligible and is likely only affected by dehydration of the apatite structure as indicated by the negative signal at ca. 1630 $cm^{-1}$. This latter signal suggests that water is removed from the RuHAp/cyclohexane interface and confirms that the RuHAp film is still hydrated prior to admittance of the alcohol solution.

**Table 1**
Vibrational modes assignment in the 1900–1200 $cm^{-1}$ spectral region at 60 °C for species present under oxidation conditions on RuHAp

| Species | Frequency ($cm^{-1}$) | Assignment |
|---|---|---|
| Surface $RuO_x(OH)_2$ phase | 1863 | $2\nu(Ru^{n+}–O)$ oxidized |
| | 1822 | $2\nu(Ru^{n+}–O)$ reduced |
| Adsorbed water | 1630 | $\delta$(O–H) |
| Benzyl alcohol | 1583 | $\nu$(C=C) + $\delta$(C–H), ring |
| | 1497 | $\delta$(C–H) + $\nu$(C=C), ring |
| | 1395 | $\delta$(O–H) |
| Benzaldehyde | 1713 | $\nu(C–O)_{sol}$ |
| | 1690 | $\nu(C=O)_{ads}$ |
| | 1599 | $\nu$(C=C) + $\delta$(C–H), ring |
| | 1583 | $\nu$(C=C) + $\delta$(C–H), ring |
| | 1316 | $\delta$(C–H) + $\nu$(C=C), ring |
| $CO_3^{2-}$ | 1657 | $\nu$(COO) bidentate |
| | 1622 | $\nu$(COO) bidentate |
| | 1599 | $\nu$(COO) mono–bidentate |
| | 1583 | $\nu$(COO) mono–bidentate |
| | 1551 | $\nu$(COO) monodentate |
| | 1417 | $\nu$(COO) monodentate |
| | 1316 | $\nu$(COO) bidentate |
| $HCO_3^-$ | 1688 | $\nu$(COO) |
| | 1657 | $\nu$(COO) |
| | 1622 | $\nu$(COO) |
| | 1266 | $\delta$(COH) |

The formation of the desired partial oxidation product benzaldehyde is also detected despite the low intensity of the carbonyl signal at 1713 $cm^{-1}$. The bands associated with dissolved benzaldehyde appear with significant intensity only during the oxidative phase and under stopped-flow conditions (Fig. 1b). Under these conditions the spectra are complicated by an additional set of signals in the 1700–1300 $cm^{-1}$ spectral range.

The observation of dissolved benzaldehyde is crucial because it enables the correlation between catalytic activity and the changes observed in the ATR-IR spectra. However, the slower reaction rate in cyclohexane, combined with the low amount of catalyst (ca. 5 mg), rendered impossible a quantification of the extent of conversion within the ATR cell under flow conditions. Batch test reactions have ensured that the use of cyclohexane does not affect the catalytic process in terms of products distribution compared to toluene; however the overall reaction rate was decreased, the conversion values decreasing from 99 to 45% after 1 h reaction time, when changing from toluene to cyclohexane.

The overtone signals of the $Ru^{n+}$–O stretching vibrations at 1863 and 1822 $cm^{-1}$ [44] allow the monitoring of the structural changes of the catalyst surface during the reaction simultaneous to the detection of dissolved and adsorbed reactant and product species. These signals correspond to those observed previously using DRIFT [27] and are attributed to the hydrated $RuO_x$ phase. The strong intensity variations associated with them indicate a reduction process involving the hydrated $RuO_x$ phase in the presence of benzyl alcohol. The classic mechanism also proposed for alcohol oxidation on RuHAp [45–48] involves two dehydrogenation steps. The extent of interaction between the generated hydrogen and the Ru should not be associated with reduction to metallic Ru, as indicated by EXAFS [16] and is therefore better interpreted as a transformation from hydrated to dehydrated or even hydrogenated $RuO_x$-like phase. In fact, a Ru hydride has been postulated as a reaction intermediate [16].

The alternate exposure of the catalyst to oxidizing (air-saturated solvent) and reducing ($H_2$-saturated solvent) conditions in the concentration modulation approach offers a more detailed insight into the redox behavior of this oxidic surface phase immersed in the liquid phase. The method is based on the periodic stimulation of the system by perturbation of an experimental parameter, such as the reactant concentration. The potential of the method lies in the enhancement of the signal-to-noise ratio, so that analytical signals

of intensity down to micro absorbance units are detectable, and in the resolution of overlapping bands related to species responding to the applied periodic perturbation with different kinetics [41].

The phase-resolved spectra (Fig. 1c) of the *in situ* oxidation–reduction ATR-IR experiment clearly show that the structure of the surface $RuO_x$ aggregates follows the applied stimulation. For instance, the overtone signals at 1863 and 1822 $cm^{-1}$ appear in exact antiphase (180° difference phase angle), indicating that the surface oxidic phase is reversibly reduced and oxidized to some extent (likely not to metallic Ru). Furthermore, the surface water content increases during the $O_2$-rich half-period, being the phase of the 1629 $cm^{-1}$ signal close to that of the signal at 1863 $cm^{-1}$. Interestingly, in the OH-stretching region (not shown) a broad feature centered at ca. 3600 $cm^{-1}$ behaves in antiphase with the signal at 1822 $cm^{-1}$, indicating that when reduction occurs the amount of free OH groups decreases.

The presence and the reducibility of the $RuO_x$ phase are peculiar of the RuHAp material. Such spectral features are not detected with comparable intensity when benzyl alcohol oxidation is performed on $Ru/Al_2O_3$. Similarly, the same reduction–oxidation modulation experiment shown in Fig. 1c performed on $Ru/Al_2O_3$ does not afford the same effect and longer modulation periods (longer than 10 min!) are required to observe finite changes. It is likely that Ru forms on alumina stable and well-defined metal nanoparticles with three-dimensional structure. In contrast, Ru on hydroxyapatite seems to exhibit a variety of Ru species, whose predominant fraction is likely arranged in two-dimensional $RuO_x$ aggregates. This conclusion is supported by the features observed in the STEM image exhibiting Ru-containing features of ca. 2–3 nm size (Fig. 1a). It is difficult to compare the $RuO_x$ structure associated with the signals at 1863 and 1822 $cm^{-1}$ with the single-site structure obtained from EXAFS [15,16,21]. We wonder whether small scale (up to 3 nm, STEM) two-dimensional aggregates would not be more suitable to describe the hydrated $RuO_x$ phase. The basicity of the hydroxyapatite may promote the formation of the hydrated phase over the Ru nanoparticles of $Ru/Al_2O_3$. Note that for ATR-IR experiments both RuHAp and $Ru/Al_2O_3$ powder films have been prepared from water suspensions and that both were therefore hydrated prior to the spectroscopic investigation. In the viewpoint of structure–activity relationships, the presence of this specific surface oxidic phase could be the reason for the enhanced performance shown by Ru-exchanged HAp [17].

That different Ru species exist on RuHAp is supported by CO adsorption experiments affording spectra containing a complex set of overlapping signals, due to the variety of surface Ru ionic and oxidic species [44,49,50]. The spectra of CO adsorbed from the liquid phase (cyclohexane) on the pristine catalyst show a complex envelope with signals at 2056, 2026, 1997, 1951 $cm^{-1}$ and shoulders at 2125 and 1885 $cm^{-1}$ (Fig. 2b). During the adsorption process the feature at 1860 $cm^{-1}$ appears as a negative band, indicating that also CO is able to reduce the surface $RuO_x$ phase to a certain extent.

The ATR-IR spectra recorded during gas phase adsorption of CO on RuHAp, i.e. in the absence of cyclohexane solvent (Fig. 2a), compare well in terms of signals shape and relative intensity with the previous DRIFT data [27] but are located at lower frequency by ca. 10 $cm^{-1}$. These shifts are related to a probable influence on the position of the CO signals of the adsorbed water molecules remaining after preparation of the particulate film for the ATR-IR measurements [36]. It should be noted that in contrast to these measurements, the materials studied using DRIFT were not pretreated, though containing adsorbed water. A shift is also observed between the spectra recorded in the ATR mode from gas- (Fig. 2a) and liquid-phase (Fig. 2b). The shift could be attributed to the same effect but cyclohexane shows a lesser degree of interference compared to water due to a weaker interaction with Ru.

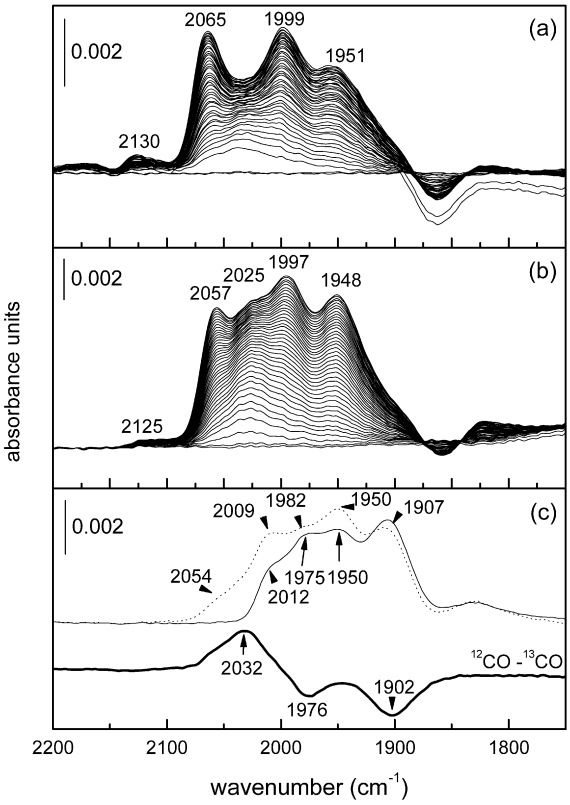


**Fig. 2.** Time-dependent ATR-IR spectra during (a) gas-phase and (b) liquid-phase CO adsorption on RuHAp. (c) ATR-IR spectra after 2 h *in situ* $^{13}CO$ adsorption on RuHAp (thin line) and upon following 1 h exchange with $^{12}CO$ till equilibrium (dotted lined) and their difference spectrum (thick line) obtained by subtracting the latter spectrum from the former one. Conditions: cyclohexane solvent, 10% $^{12}CO$/Ar, $^{13}CO$, 333 K, 0.6 ml/min flow rate, 2 h.

In both gas- and liquid-phase adsorption, the signals grow rather slowly if compared with the adsorption onto reduced $Ru/Al_2O_3$ [36] and therefore on nanosized metallic Ru. Comparison of Figs. 2a and 2b reveals differences in overall and relative intensity. For example, the spectrum obtained after 2 h CO adsorption from the liquid-phase resembles that recorded after 1 h adsorption from gas-phase. Therefore, adsorption seems to occur more slowly if CO is supplied from the saturated solvent than from the gas phase, probably as a combined consequence of a lower actual concentration of the gas in cyclohexane and of a diminished surface availability (competition between CO and solvent). However, the fact that the adsorption kinetic is slow in both cases suggests that CO adsorption may induce surface restructuring to some extent, which is reflected in the changes of the signal at 1860 $cm^{-1}$. Phenomena of partial reduction or oxidative disruption of metal particles are known to occur for Ru and Rh based materials exposed to CO in the presence of surface hydroxyl groups promoting the process [44,49,51–53]. Although this has to be further proven, the apatite may potentially favor this process, indicating that the interaction between the Ru-phase and the support is significant.

On the basis of the above considerations and by comparison with the DRIFT data [27], the infrared signals in the CO region can be associated with tricarbonyl (2125 and 1951 $cm^{-1}$) and monocarbonyl (2025 $cm^{-1}$) species of ionic Ru on the $RuO_x$ phase denoted as $(RuO_x)Ru^{n+}(CO)_3$ and $(RuO_x)Ru^{n+}CO$, respectively, and with bicarbonyl species (2056 and 1995 $cm^{-1}$) on the poorly accessible $Ru^{3+}$ ions in the channels of the HAp structure, denoted as $Ru^{3+}(CO)_2$. The monocarbonyl species appear to be populated first. It is also clear that no feature observed in Fig. 2 can be associated with reduced Ru [27].

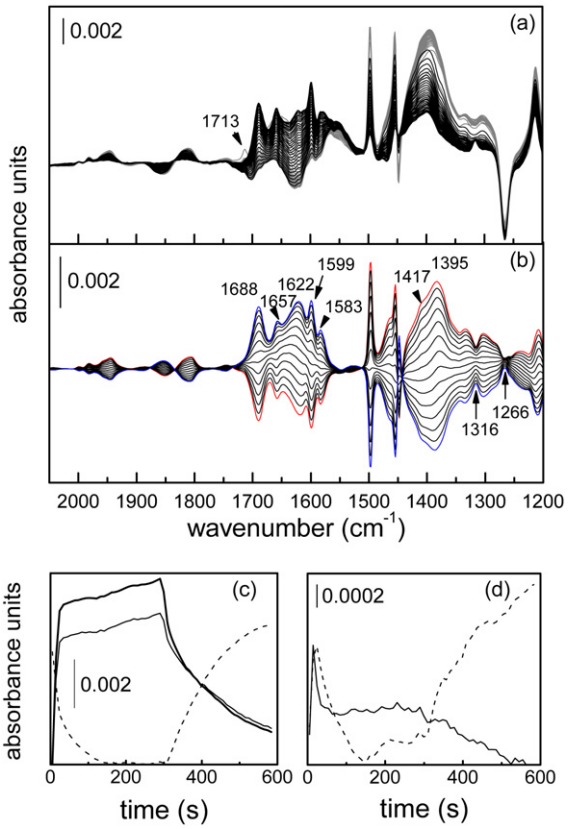


**Fig. 3.** (a) ATR-IR spectra obtained during a MES experiment in which the feed was periodically switched between alcohol (gray spectra) and $O_2$-saturated solvent (black spectra) and (b) the corresponding phase-resolved spectra with 10° phase angle difference. (c) Time-dependent profiles for peaks maxima at 1395 (thick line), 1417 (thin line) and 1688 $cm^{-1}$ (dashed line), and (d) at 1713 (thin line) and 1857 $cm^{-1}$ (dashed line). Conditions: cyclohexane solvent, benzyl alcohol 0.02 M, $O_2$, 333 K, 0.6 ml/min flow rate.

$^{13}CO$ adsorption affords a spectral pattern comparable to the one shown above for $^{12}CO$ but red shifted by ca. 40 $cm^{-1}$ (Fig. 2c, thin line), in agreement with the isotopic effect. The time-dependent ATR-IR spectra recorded while admitting the $^{12}CO$-saturated solvent indicate that the exchange is only partial and show the signals of $^{13}CO$ still coexisting with the new bands arising from $^{12}CO$ (Fig. 2c, dotted line). The difference spectrum between the $^{12}CO$-rich phase and the $^{13}CO$-rich phase (Fig. 2c, thick line) exhibits a clear positive signal at 2032 $cm^{-1}$ and seems to suggest that the exchange occurs mainly for the species denoted as monocarbonyl present on the $RuO_x$ phase.

The information collected so far, i.e. the observed changes in the signals related to the $RuO_x$ phase under reducing/oxidizing conditions and in the presence of CO, provides evidence on how significantly the $RuO_x$ phase participates in the interfacial processes. In particular Ru-sites associated with monocarbonyl species appears highly susceptible to the environment.

Fig. 1 showed that benzaldehyde is produced when benzyl alcohol is admitted to the spectroscopic reactor cell. However, some limitations to characterize the catalytic activity and its relation with the surface species appear under flow conditions. In order to increase the sensitivity of the infrared technique and therefore better elucidate the nature of the species present on the catalyst surface under conditions relevant to catalysis, MES measurements have been performed by periodically changing the concentration of the alcohol (between 0 and 20 mM) under (constant) oxidative conditions. The phase-resolved spectra and the time-dependent profiles of selected signals are reported in Fig. 3. The phase-resolved spectra clearly show the higher resolution that can be

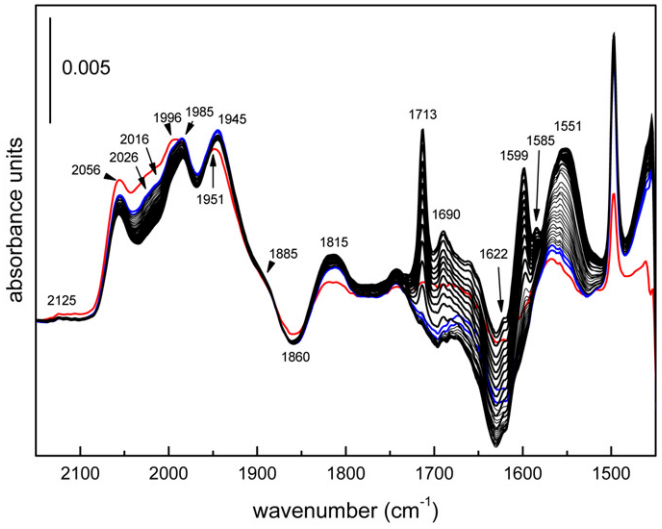


**Fig. 4.** ATR-IR spectra of a solution of benzyl alcohol under oxidative conditions ($O_2$) on RuHAp preequilibrated with CO (2 h, red spectrum). Blue spectra refer to the early stages of the flow reaction conditions, thin black spectra to the flow reaction conditions and thick black spectra to the following stopped-flow conditions. Conditions: cyclohexane solvent, benzyl alcohol 0.02 M, 10% $^{12}CO$/Ar, 333 K, 0.6 ml/min flow rate. (For interpretation of the references to color in this figure legend, the reader is referred to the web version of this article.)

obtained with the technique, by filtering out the strong contribution of static signals. The intensity profiles (Figs. 3c–3d) evidence that as soon as the alcohol is admitted to the cell, benzaldehyde (1713 $cm^{-1}$) is formed and the $RuO_x$ phase (1856 $cm^{-1}$) is reduced. We cannot provide any evidence for the formation of a hydride intermediate but its presence may be supported by the rapid reduction of the $RuO_x$-phase in contact with benzyl alcohol. Despite the improved sensitivity of the infrared technique, signals of the Ru–H stretching mode in the 1970–1870 spectral range [54–57] have not been detected, likely due to the very low concentration and short life time of the hydrido-Ru species and to the significant overlap with the alcohol signals.

When oxygen contacts the catalyst, Ru is re-oxidized (as in Fig. 1) and a set of signals appears in the 1700–1200 $cm^{-1}$ spectral region (Fig. 3a). These signals may indicate that the increase of the water content on the surface (large signal between 1657 and 1622 $cm^{-1}$) under reaction conditions affords $HCO_3^-$ species from hydration of the carbonate species permanently incorporated in the apatite structure during synthesis and exposure to air [58], whereas under oxidative conditions the hydrogenocarbonates formed (1688 $cm^{-1}$) are transformed back into carbonates and water. Complementary experiments, using $^{13}C$-labeled benzyl alcohol [32], exclude that carbonates and hydrogenocarbonates originate from CO formation from benzaldehyde decomposition, which was observed on $Pd/Al_2O_3$ [42,59].

A closer look at the phase-resolved spectra allows recognizing a shoulder at 1417 $cm^{-1}$, which is slightly out of phase (retarded evolution) with respect to the broad feature of the alcohol (1395 $cm^{-1}$). This band, already present in the DRIFT spectrum of the pristine catalyst (not shown), is unambiguously attributed to carbonate species [43]. Therefore, alcohol and carbonate species possess slightly different kinetic. It is worth noting that the feature attributed to the carbonates and the signal due to the hydrogenocarbonates species (for example, 1688 $cm^{-1}$) are in antiphase, meaning that the carbonate hydration process is completely reversible and that species can be most likely stored on the apatite surface during reaction.

Fig. 4 displays the spectra obtained when preadsorbing CO on RuHAp followed by reaction as described above (flow and stopped-flow). Already in the early spectra, the competition for adsorption

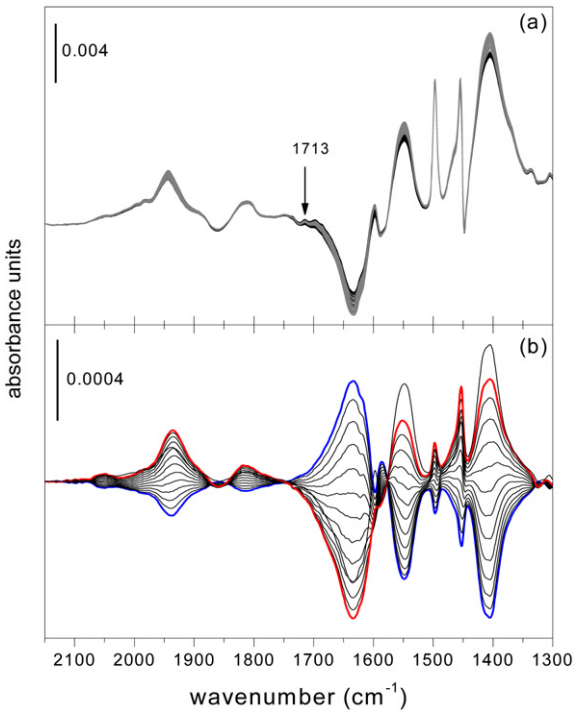


**Fig. 5.** ATR-IR spectra during a MES experiment in which the feed was periodically switched between reaction mixture and a CO-saturated alcohol solution. (a) Time-dependent spectra (gray, the $O_2$-rich phase; black, the CO-rich phase) and (b) the corresponding phase-resolved spectra with 10° phase angle difference. Conditions: cyclohexane solvent, benzyl alcohol 0.02 M, 10% $^{12}$CO/Ar, 333 K, 0.6 ml/min flow rate.

sites between CO and the alcohol produces a significant decrease in intensity of the carbonyl signals at high frequency and an increase in the absorption at 1945 $cm^{-1}$. Beside competition, this behavior may also find origin in a partial site restructuring, since the $RuO_x$ phase is in fact further reduced in contact with the alcohol as indicated by the changes in the signals at 1860 and 1815 $cm^{-1}$. The observed phenomena of carbonyl species displacement or redistribution can be more clearly related to the catalytic activity under simulated batch conditions. Under stopped-flow conditions, the signals of benzaldehyde, carbonates and hydrogenocarbonates are more clearly visible and the feature at 2026 $cm^{-1}$, attributed to Ru-monocarbonyl species on $RuO_x$ weakens considerably, indicating that its attenuation is correlated with the appearance of the signals below 1750 $cm^{-1}$, including that of dissolved benzaldehyde.

Supporting information is gained when the reaction mixture is admitted to the pristine catalyst alternately to the CO-saturated alcohol solution. Hence, CO interacts with the catalyst surface at work. The time-resolved spectra (Fig. 5a, black) show very similar features to those found in Fig. 1 and the repetitive change between the two solutions causes only minor changes. Additionally, the signal at 1937 $cm^{-1}$ is certainly due to CO adsorbed on Ru sites. As benzaldehyde can be distinguished, the spectra can be again related to the catalyst at work. The spectra also contain information on the species observed previously and related to carbonates (1550 and 1417 $cm^{-1}$) [43]. This is clearer in Fig. 5b in the phase-resolved spectra of the same experiment. These spectra provide information only on the signals (species) that are reversibly affected by the change between oxygen-saturated and CO-saturated alcohol solution. A closer look at these spectra shows that the aldehyde production is only partially inhibited under the CO-rich phase. Simultaneously, CO adsorbs affording a signal at 1937 $cm^{-1}$. This feature appeared during CO adsorption (Fig. 2) and was responsible, together with a band at 1971 $cm^{-1}$, of an asymmetric broadening of the signals in the low energy region (<2000 $cm^{-1}$). It is generally assigned to the monocarbonyl form of CO linearly bonded to ruthenium in different oxidation states, $Ru^{n+}O_x(CO)$, in the present case probably indicating the presence of $Ru^{n+}$ entities in $RuO_x$ ($x < 2$) clusters [53,60]. Therefore, this signal does not belong to the same multicarbonyl species exhibiting signals at 2056 and 1997 $cm^{-1}$ and is less relevant for the catalytic process. The absence of high frequency signals suggests that the Ru sites located on the $RuO_x$ phase may contribute to the oxidation of benzyl alcohol in agreement with the spectra shown in Fig. 4. Formation of carbonate species (1550 and 1417 $cm^{-1}$) is promoted in the CO-rich phase, likely as a consequence of direct CO oxidation to $CO_2$. In contrast to the spectra in Figs. 1, 3 and 4, $HCO_3^-$ species are not detected in time- and phase-resolved spectra. An important difference between Figs. 3 and 5 is that the alcohol reactant is continuously supplied in the experiment of Fig. 5 and that the hydrogenocarbonate species form when the alcohol is removed from the cell (Fig. 3b). Hence, it is tempting to associate the sites where such species are formed with sites where the reaction takes place. Although this observation is rather speculative, together with the fact that a hydrated site may be involved in $HCO_3^-$ formation, it may reveal that alcohol oxidation in fact requires hydrated Ru species as that represented by the 1863–1822 $cm^{-1}$ overtone signals.

On the basis of all the evidences so far collected, some more detailed considerations concerning the oxidation mechanism are proposed. As recalled above, the chemical nature of the active ruthenium species and the mechanism of the oxidation of alcohols on Ru-hydroxyapatite based catalysts have been investigated by *in situ* EXAFS and kinetic analysis [16,17]. The suggested mechanism involves the formation of a Ru-alcoholate species, which undergoes $\beta$-hydride elimination to produce the carbonyl compound and an hydrido-ruthenium intermediate species, then reoxidized by molecular oxygen, thus closing the catalytic cycle.

Given the changes observed in the spectra presented here and the reactivity of the $RuO_x$-phase associated with the overtone signals at ca. 1850 $cm^{-1}$, the participation of the hydrated $Ru^{n+}$ species onto the $RuO_x$ phase can be considered more crucial than that of the isolated Ru ionic species on the HAp surface and in the channel structure. In fact, no significant changes have been observed that are correlated to these latter species. That the hydrido-species proposed as intermediate in the alcohol oxidation exists and belongs to the hydrated $RuO_x$-like phase is difficult to ascertain. However, it may easily be formed there as indicated by the changes in the overtone region of the Ru–O signal (Fig. 1c) and in the OH-stretching region where the concentration of OH groups appears to decrease, suggesting a possible correlation with a reduced species as the HO–Ru($O_2$)–H hydrido species.

Besides the presence of the substrate, the carbonyl product and water, signals related to carbonates and hydrogenocarbonates species have been observed (Fig. 1b). These species may be regarded as not directly participating into the reaction mechanism that is as spectators. Although, it is likely that $CO_3^{2-}$ and especially $HCO_3^-$ are preferentially stored on sites related to the fate of benzyl alcohol (vide infra), their formation and storage do not appear to inhibit the desired oxidation of the alcohol upon progressive blocking surface adsorption sites. A closer look at time dependent spectra collected under stopped flow reaction conditions (not shown) allows evidencing that the rate of formation of these species follows the same time-scale as that of benzaldehyde production. Furthermore, the reversible interconversion between hydrogenocarbonates and carbonates suggests that their surface concentration remains unchanged in a catalytic cycle.

## 4. Conclusions

The fate of Ru species in RuHAp during the aerobic oxidation of benzyl alcohol has been elucidated by means of *in situ* ATR-IR spectroscopy. Simultaneous monitoring of surface and dissolved species under working conditions provided evidences for various surface processes occurring during the aerobic alcohol oxidation. The major findings can be summarized as follows:

- The marked intensity changes of the pattern attributed to the surface $RuO_x$ phase (1860 $cm^{-1}$) under oxidation–reduction cycles clearly indicate its redox properties and participation in the interfacial processes.
- The *in situ* CO adsorption provides evidence for surface Ru species of the type $(RuO_x)Ru^{n+}(CO)_3$, $(RuO_x)Ru^{n+}CO$ (hydrated $RuO_x$ phase) and $Ru^{3+}(CO)_2$.
- The exchange of $^{13}C$ isotopically labeled carbonyl ligands upon admission of $^{12}CO$ seems to occur more easily for the Ru monocarbonyl species located on the $RuO_x$ phase.
- Upon admission of the reaction mixture, some degree of reduction of the $RuO_x$ surface phase occurs simultaneously to the appearance of the partial oxidation product (benzaldehyde).
- Infrared signals attributed to surface water, hydrogenocarbonates and carbonates species occur under oxidative conditions.
- The carbonate hydration process affording hydrogenocarbonates seems to be reversible and to occur in the presence of the hydrated $RuO_x$ phase. Furthermore, the presence of benzyl alcohol inhibits this surface reaction, likely competing for the same sites.
- That a particularly active species, i.e. the Ru-hydride intermediate, is formed under reaction conditions cannot be concluded from the present data.
- The admission of benzyl alcohol to a CO saturated surface mainly frees the adsorption sites for monocarbonyl Ru species associated with the surface $RuO_x$ phase; simultaneously the aldehyde signals are detected.
- Inversely, CO admitted in the presence of the alcohol does not adsorb on Ru species supported on the $RuO_x$ phase.

These observations correlating information on the catalyst structure and the surface reactivity support the suggestion that the hydrated $Ru^{n+}$-oxide phase is the active phase for benzyl alcohol oxidation, while carbonates and hydrogenocarbonates are identified as spectator species on the catalyst surface.

## Acknowledgments

The authors gratefully acknowledge the financial support from the Foundation Claude and Giuliana. Dr. R. Wirz is thanked for providing support with the use of the demodulation function and Dr. F. Krumeich for the STEM images.

## References

[1] S. Sugiyama, T. Shono, D. Makino, T. Moriga, H. Hayashi, J. Catal. 214 (2003) 8.
[2] K. El Kabouss, M. Kacimi, M. Ziyad, S. Ammar, A. Ensuque, J.Y. Piquemal, F. Bozon-Verduraz, J. Mater. Chem. 16 (2006) 2453.
[3] M.P. Reddy, A. Venugopal, M. Subrahmanyam, Appl. Catal. B 69 (2007) 164.
[4] K. El Kabouss, M. Kacimi, M. Ziyad, S. Ammar, F. Bozon-Verduraz, J. Catal. 226 (2004) 16.
[5] N. Cheikhi, M. Kacimi, M. Rouimi, D. Ziyad, L.F. Liotta, G. Pantaleo, G. Deganello, J. Catal. 232 (2005) 257.
[6] B.M. Choudary, C. Sridhar, M.L. Kantam, B. Sreedhar, Tetrahedron Lett. 45 (2004) 7319.
[7] Y. Maeda, Y. Washitake, T. Nishimura, K. Iwai, T. Yamaguchi, S. Uemura, Tetrahedron 60 (2004) 9031.
[8] Z. Boukha, M. Kacimi, M. Ziyad, A. Ensuque, F. Bozon-Verduraz, J. Mol. Catal. A Chem. 270 (2007) 205.
[9] S. Sugiyama, S. Tanimoto, K. Fukuda, K. Kawashiro, T. Tomida, H. Hayashi, Colloids Surf. A 252 (2005) 187.
[10] M. Wakamura, K. Kandori, T. Ishikawa, Colloids Surf. A 164 (2000) 297.
[11] M. Wakamura, K. Kandori, T. Ishikawa, Colloids Surf. A 142 (1998) 107.
[12] R. Tahir, K. Banert, A. Solhy, S. Sebti, J. Mol. Catal. A Chem. 246 (2006) 39.
[13] A. Solhy, J.H. Clark, R. Tahir, S. Sebti, M. Larzek, Green Chem. 8 (2006) 871.
[14] Z. Opre, J.D. Grunwaldt, M. Maciejewski, D. Ferri, T. Mallat, A. Baiker, J. Catal. 230 (2005) 406.
[15] K. Yamaguchi, K. Mori, T. Mizugaki, K. Ebitani, K. Kaneda, J. Am. Chem. Soc. 122 (2000) 7144.
[16] Z. Opre, J.D. Grunwaldt, T. Mallat, A. Baiker, J. Mol. Catal. A Chem. 242 (2005) 224.
[17] Z. Opre, D. Ferri, F. Krumeich, T. Mallat, A. Baiker, J. Catal. 241 (2006) 287.
[18] K. Tonsuaadu, M. Gruselle, F. Villain, R. Thouvenot, M. Peld, V. Mikli, R. Traksmaa, P. Gredin, X. Carrier, L. Salles, J. Colloid Interface Sci. 304 (2006) 283.
[19] K. Mori, K. Yamaguchi, T. Mizugaki, K. Ebitani, K. Kaneda, Chem. Commun. (2001) 461.
[20] K. Mori, M. Tano, T. Mizugaki, K. Ebitani, K. Kaneda, New J. Chem. 26 (2002) 1536.
[21] K. Mori, T. Hara, T. Mizugaki, K. Ebitani, K. Kaneda, J. Am. Chem. Soc. 125 (2003) 11460.
[22] C.M. Ho, W.Y. Yu, C.M. Che, Angew. Chem. Int. Ed. 43 (2004) 3303.
[23] M. Onaka, T. Seki, Y. Masui, J. Synth. Org. Chem. Jpn. 63 (2005) 492.
[24] S. Wuyts, D.E. De Vos, F. Verpoort, D. Depla, R. De Gryse, P.A. Jacobs, J. Catal. 219 (2003) 417.
[25] K. Mori, S. Kanai, T. Hara, T. Mizugaki, K. Ebitani, K. Jitsukawa, K. Kaneda, Chem. Mater. 19 (2007) 1249.
[26] K. Mori, T. Hara, T. Mizugaki, K. Ebitani, K. Kaneda, J. Am. Chem. Soc. 126 (2004) 10657.
[27] Z. Opre, D. Ferri, F. Krumeich, T. Mallat, A. Baiker, J. Catal. 251 (2007) 48.
[28] N.J. Harrick, Internal Reflection Spectroscopy, Interscience, New York, 1967.
[29] T. Bürgi, A. Baiker, Adv. Catal. 50 (2006) 227.
[30] T. Bürgi, J. Catal. 229 (2005) 55.
[31] R. Wirz, D. Ferri, A. Baiker, Langmuir 22 (2006) 3698.
[32] D. Ferri, C. Mondelli, F. Krumeich, A. Baiker, J. Phys. Chem. B 110 (2006) 22982.
[33] I. Dolamic, T. Bürgi, J. Phys. Chem. B 110 (2006) 14898.
[34] C. Mondelli, D. Ferri, J.D. Grunwaldt, F. Krumeich, S. Mangold, R. Psaro, A. Baiker, J. Catal. 252 (2007) 77.
[35] I. Ortiz-Hernandez, C.T. Williams, Langmuir 23 (2007) 3172.
[36] A.S. Baird, K.M. Kross, D. Gottschalk, E.A. Hinson, N. Wood, K.A. Layman, J. Phys. Chem. C 111 (2007) 14207.
[37] S.D. Ebbesen, B.L. Mojet, L. Lefferts, Langmuir 24 (2008) 869.
[38] T. Bürgi, R. Wirz, A. Baiker, J. Phys. Chem. B 107 (2003) 6774.
[39] D. Baurecht, U.P. Fringeli, Rev. Sci. Instrum. 72 (2001) 3782.
[40] T. Bürgi, A. Baiker, J. Phys. Chem. B 106 (2002) 10649.
[41] D. Baurecht, I. Porth, U.P. Fringeli, Vib. Spectrosc. 30 (2002) 85.
[42] C. Keresszegi, D. Ferri, T. Mallat, A. Baiker, J. Phys. Chem. B 109 (2005) 958.
[43] S. Koutsopoulos, J. Biomed. Mater. Res. 62 (2002) 600.
[44] K. Hadjiivanov, J.C. Lavalley, J. Lamotte, F. Mauge, J. Saint-Just, M. Che, J. Catal. 176 (1998) 415.
[45] K. Ebitani, H.B. Ji, T. Mizugaki, K. Kaneda, J. Mol. Catal. A Chem. 212 (2004) 161.
[46] I.W.C.E. Arends, T. Kodama, R.A. Sheldon, Top. Organomet. Chem. 11 (2004) 277.
[47] B.Z. Zhan, M.A. White, T.K. Sham, J.A. Pincock, R.J. Doucet, K.V.R. Rao, K.N. Robertson, T.S. Cameron, J. Am. Chem. Soc. 125 (2003) 2195.
[48] T.L. Stuchinskaya, M. Musawir, E.F. Kozhevnikova, I.V. Kozhevnikov, J. Catal. 231 (2005) 41.
[49] E. Guglielminotti, F. Boccuzzi, M. Manzoli, F. Pinna, M. Scarpa, J. Catal. 192 (2000) 149.
[50] K.I. Hadjiivanov, G.N. Vayssilov, Adv. Catal. 47 (2002) 307, and references therein.
[51] F. Solymosi, M. Pasztor, J. Phys. Chem. 89 (1985) 4789.
[52] M.I. Zaki, G. Kunzmann, B.C. Gates, H. Knözinger, J. Phys. Chem. 91 (1987) 1486.
[53] T. Mizushima, K. Tohji, Y. Udagawa, A. Ueno, J. Am. Chem. Soc. 112 (1990) 7887.
[54] M.D. Fryzuk, M.J. Petrella, R.C. Coffin, B.O. Patrick, C. R. Chimie 5 (2002) 451.
[55] M.S. Song, S.J. Kim, I.W. Shim, S.J. Oh, Y.S. Yang, H.K. Suh, React. Polym. 22 (1994) 35.
[56] G. Sbrana, G. Braca, E. Giannetti, JCS Dalton Trans. (1976) 1847.
[57] N.A. Jasim, R.N. Perutz, S.P. Foxon, P.H. Walton, JCS Dalton Trans. (2001) 1676.
[58] Z.H. Cheng, A. Yasukawa, K. Kandori, T. Ishikawa, Langmuir 14 (1998) 6681.
[59] C. Keresszegi, D. Ferri, T. Mallat, A. Baiker, J. Catal. 234 (2005) 64.
[60] N.M. Gupta, V.S. Kamble, R.M. Iyer, K.R. Thampi, M. Grätzel, J. Catal. 137 (1992) 473.